

Robust Multiple-Range Coherent Quantum State Transfer

Bing Chen^{1,2,*}, Yan-Dong Peng¹, Yong Li^{2,3}, and Xiao-Feng Qian^{4†}

¹*College of Electronics, Communication & Physics,*

Shandong University of Science and Technology, Qingdao 266510, China

²*Beijing Computational Science Research Center, Beijing 100094, China*

³*Synergetic Innovation Center of Quantum Information and Quantum Physics,
University of Science and Technology of China, Hefei, Anhui 230026, China and*

⁴*Center for Coherence and Quantum Optics, The Institute of Optics,
University of Rochester, Rochester, NY 14627, USA*

(Dated: October 29, 2018)

We propose a multiple-range quantum communication channel to realize coherent two-way quantum state transport with high fidelity. In our scheme, an information carrier (a qubit) and its remote partner are both adiabatically coupled to the same data bus, i.e., an N -site tight-binding chain that has a single defect at the center. At the weak interaction regime, our system is effectively equivalent to a three level system of which a coherent superposition of the two carrier states constitutes a dark state. The adiabatic coupling allows a well controllable information exchange timing via the dark state between the two carriers. Numerical results show that our scheme is robust and efficient under practically inevitable perturbative defects of the data bus as well as environmental dephasing noise.

PACS numbers: 03.65.-w, 03.67.Hk, 73.23.Hk

I. INTRODUCTION

Quantum state transfer (QST) in many-body solid state physical systems plays a central role in the realization of various localized quantum computation and quantum communication proposals [1, 2]. A practical high quality quantum state transfer scheme needs to possess several desirable features: i) high fidelity (to preserve the transferred message), ii) robustness (to tolerate inevitable practical errors, imperfections, and decoherence), iii) efficiency (to achieve optimal results with minimal implementations), and iv) flexibility (to serve for multiple tasks). The investigation of accomplishing high fidelity quantum state transfer in electronic and spin systems has recently drawn tremendous attention (see for example [3–16] and an overview [2]). Many of these schemes are based on the natural dynamical evolution of permanent coupled chain of quantum systems, and require no control during the QST. However, such schemes rely on precise manufacture of the system interaction parameters as well as accurate timing of information processing, and may not be robust against experimental imperfection settings, such as small variations of the system Hamiltonian, environmental noise, etc.

Recently, adiabatic passage has been paid much attention for quantum information transfer in various physical systems [17–45]. One typical way is called coherent QST which involves a quantum system that has an instantaneous eigenstate that is a superposition of a message state and its corresponding target state. Stimulated Raman adiabatic passage (STIRAP) [17] is such an example in

a three-level atomic system. In this technique, the dark state which is a coherent superposition of message and target states plays a central role in the process of information transfer. In STIRAP evolution, the message and target states are coupled to a same intermediate state by a pump pulse and a Stokes pulse respectively. If the two pulses are applied counter-intuitively, i.e., the Stokes pulse is applied before the pump, then the dark state is associated initially with the message state and eventually with the target state. Such a process effectively transports the information of the message state to the desired target state. There are a couple of advantages of the adiabatic passage scheme: it is robust against small errors and imperfections of settings, and the QST timing can be controlled freely and precisely.

In this paper we extend the STIRAP protocol to an N -site tight-binding model and show that it is suitable for high fidelity robust multiple-range QST and quantum information swapping (see schematic illustration in Fig. 1). The tight-binding quantum dot (QD) array with a single diagonal defect serves as the adiabatic pathway for two-way electronic transport. Two external QDs A, B represent information sender and receiver or vice versa are allowed to be flexibly side coupled to the array (i.e., QDs A B can couple to different sites of the QD array as required by particular tasks). In this scheme, the coupling parameters between the external QDs and the corresponding sites on the array are made time dependent, which are controlled by the sender and receiver, respectively. We find that the ground state of the array is a bound state (or localized state) due to the existence of the defect. This allows us to show analytically that our system is an effective three-level system when the coupling between QD A (B) and the QD array are weak. As a consequence it is demonstrated that high fidelity two-way QST can be realized at various different distances

*Electronic address: chenbingphys@163.com

†Electronic address: xfqian@pas.rochester.edu

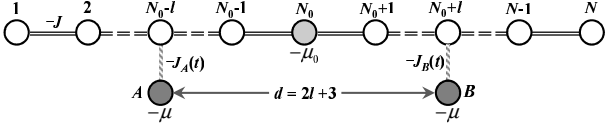


FIG. 1: Schematic illustrations of multiple-range adiabatic quantum state transfer from A to B. The tight-binding array with single defect is acting as a quantum data bus, in which the coupling strengths $-J$ are time-independent and the defect QD is supplied with energy $-\mu_0$. The sender (QD A) and the receiver (QD B) supplied with on-site energy, $-\mu$ are coupled to two sites of the array on opposite sides with respect to the defect site. The sender controls $-J_A(t)$ and the receiver controls $-J_B(t)$. The transfer distance in terms of the number of sites is given as $d = 2l + 3$.

between the sender and receiver. Numerical results are also performed to illustrate that our scheme is robust against dephasing and small variations of the QD couplings and imperfections.

The paper is organized as follows. In Sec. II, the driven model is described and the tight-binding QD array system is analyzed in detail. In Sec. III, the multiple-range adiabatic transport scheme and its effective Hamiltonian are discussed analytically. A practically imperfect model, as well as an open dephasing model are considered numerically. The last section summarizes the paper.

II. DRIVEN MODEL

We start here with the structure of our proposal illustrated in figure 1: the channel connecting the two side QDs A and B is a one-dimensional tight-binding array with uniform and always-on exchange interactions and with one diagonal defect at N_0 th site. The coupling between the QDs A, B and their corresponding channel sites are made time dependent. The total Hamiltonian can be written in the following structure:

$$\hat{\mathcal{H}} = \hat{\mathcal{H}}_M + \hat{\mathcal{H}}_{AB} + \hat{\mathcal{H}}_I \quad (1a)$$

$$\hat{\mathcal{H}}_M = -\hbar J \sum_{j=1}^{N-1} (|j\rangle \langle j+1| + \text{h.c.}) - \mu_0 |N_0\rangle \langle N_0| \quad (1b)$$

$$\hat{\mathcal{H}}_{AB} = -\mu (|A\rangle \langle A| + |B\rangle \langle B|) \quad (1c)$$

$$\hat{\mathcal{H}}_I = -\hbar J_A(t) |A\rangle \langle N_0-l| - \hbar J_B(t) |B\rangle \langle N_0+l| + \text{h.c.}, \quad (1d)$$

where $-J (< 0)$ is the coupling strength between nearest neighboring QDs along the channel; $J_A(t)$ is the time dependent coupling strength between A and the (N_0-l) th site of the QD array and is controlled by the sender, while $J_B(t)$ is the receiver controlled coupling strength between B and site (N_0+l) ; $-\mu_0$ and μ are the on-site energy applied on the QDs; $|j\rangle = c_j^\dagger |0\rangle$ represents the Wannier state localized in the j -th quantum site for $j = A, 1, 2, \dots, N, B$. For convenience, we consider the channel containing an odd number of QDs and

the gate voltage $-\mu_0$ is applied on the central dot, i.e. $N_0 = (N+1)/2$. Note that equation (1) comprises three terms: the first corresponds to the tight-binding chain with defect at N_0 -site, the second is the energy of QDs A, B, and the third term describes the interaction Hamiltonian. In this paper we study the electron transfer from QD-A to QD-B through the tight-binding array serving as quantum data bus, and we denote the transfer distance $d = 2l + 3$. In this proposal the propagation of the electron is driven by two time-dependent coupling strengths, i.e., $J_A(t)$ and $J_B(t)$, which are modulated in sinusoidal pulses

$$J_A(t) = J_0 \sin^2\left(\frac{\pi t}{2t_{\max}}\right), \quad (2a)$$

$$J_B(t) = J_0 \cos^2\left(\frac{\pi t}{2t_{\max}}\right), \quad (2b)$$

where t_{\max} is the prescribed duration of QST; J_0 is the maximum tunnelling rates between the two external QD and the defected chain. These two pulses are illustrated in Fig. 2(a).

Firstly, let us perform a detail analysis of the peculiar properties of the chain with single defect when used as a quantum channel for quantum state transfer. Note that the Hamiltonian $\hat{\mathcal{H}}_M$ is equivalent to a tight-binding problem with single diagonal impurity at site N_0 . Let $\{|\lambda_n\rangle\}$ and $\{\lambda_n\}$ with $n = 1, 2, \dots, N-1$ be the sets of the eigenstates of $\hat{\mathcal{H}}_M$, respectively. Then, $\hat{\mathcal{H}}_M$ can be rewritten to be

$$\hat{\mathcal{H}}_M = \sum_{n=0}^{N-1} \lambda_n |\lambda_n\rangle \langle \lambda_n|. \quad (3)$$

For $\mu_0 = 0$, the eigenstates are $|\lambda_n\rangle = \sum_{j=1}^N \sin[(n+1)\pi j/(N+1)] |j\rangle$ with energies $\lambda_n = 2J \cos[(n+1)\pi/(N+1)]$, and where $n = 0, 1, 2, \dots, N-1$. For non-zero μ_0 , we write the state in the single-particle Hilbert space as $|\lambda_n\rangle = \sum_{j=1}^N u_n(j) |j\rangle$. To see more precisely what happens for $\mu_0 \neq 0$, we solve the discrete-coordinate Schrödinger equation

$$-J[u_n(j-1) + u_n(j+1)] = (\mu_0 \delta_{j,N_0} + \lambda_n) u_n(j), \quad (4)$$

where $j \in [2, N-1]$. At the boundaries, we get slightly different equations: $-J u_n(2) = \lambda_n u_n(1)$ and $-J u_n(N-1) = \lambda_n u_n(N)$.

It is well known that the δ -type diagonal defect contributes exactly one bound state of single particle case. To solve above equations, we assume a usual solution by taking the mirror symmetry into consideration

$$u_n(j) \propto \begin{cases} \sin(k_n j), & j \leq N_0 \\ (-1)^n \sin[k_n(2N_0 - j)], & j > N_0 \end{cases} \quad (5)$$

where k_n is the wave vector. By inserting this expression into equations (4) and together with boundary condition, we obtain the eigenvalues $\lambda_n = -2J \cos k_n$ in terms of wave vector k_n , which obeys

$$\cot(k_n N_0) \sin k_n = \begin{cases} 0, & n = \text{odd number} \\ \xi, & n = \text{even number} \end{cases}, \quad (6)$$

where $\xi = \mu_0/2J$.

Based on the equation (6), one can get $N - 1$ discrete real values k_n in the interval $(0, \pi)$ and *one* purely imaginary wave vector. Together with the expression $\lambda_n = -2J \cos k_n$, the eigenenergies corresponding to real wave vectors are included in the band $(-2J, 2J)$. On the other hand, the purely imaginary wave vector give rise to a out-of-band eigenenergy. Setting $k_0 = iq$ and substituting it into Eq. (6), we have $q = \ln[\xi + \sqrt{\xi^2 + 1}]$. The wave vector q yields the eigenvalue

$$\lambda_0 = -2J \cosh q = -2J \sqrt{\xi^2 + 1}. \quad (7)$$

which splits off from the band. The corresponding localized state is given by $|\lambda_0\rangle = \sum_{j=1}^N u_0(j) |j\rangle$, with

$$u_0(j) = \Lambda^{-1/2} e^{-q|N_0-j|} \quad (8)$$

where $\Lambda = \cosh q / \sinh q$.

Until now, we have only discussed the solutions of Eq. (4) without any external perturbation. In the thermodynamic limit $N_0 \rightarrow \infty$, the excited energies become a continuous energy band; it is not hard to find that the energy gap between the ground state and the first excited state (see Fig. 2(b)) is

$$\Delta = 2J \left(\sqrt{\xi^2 + 1} - 1 \right). \quad (9)$$

III. ADIABATIC TRANSPORT SCHEME

A. Effective Hamiltonian

We now turn our attention to derive the effective Hamiltonian of the total system when the couplings between QDs A, B (sender and receiver) and the tight-binding QD array are weak. In the absence of the coupling between the QDs A, B and the QD array ($J_A = J_B = 0$) the ground states of the total Hamiltonian (1) are threefold degenerate for one electron problem by setting $\mu = 2J \sqrt{\xi^2 + 1}$, i.e., the states $|A\rangle$, $|\lambda_0\rangle$, and $|B\rangle$ have the same energy $-\mu$. According to Eq. (2a) and (2b), The time-dependent tunnelling rates J_A and J_B are varied in the interval $[0, J_0]$ as time process from 0 to t_{\max} . We assume the couplings between two side QDs

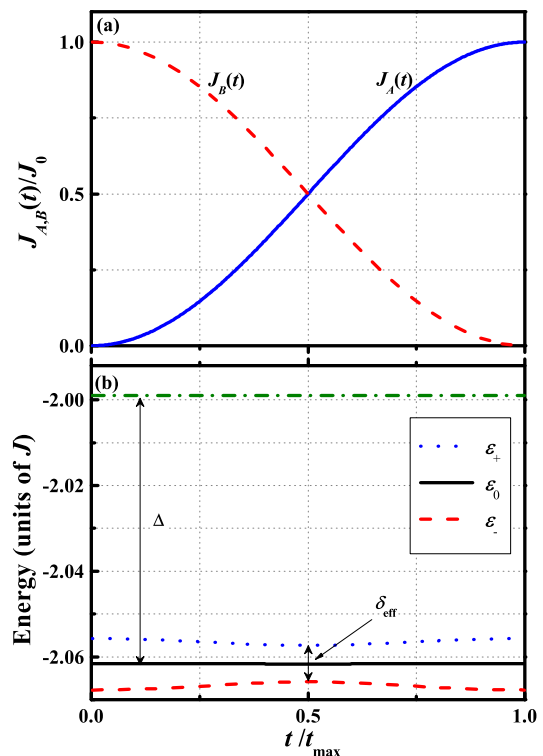


FIG. 2: (Color online) (a) The time-dependent tunnelling rates $J_A(t)$ and $J_B(t)$ as a function of time (in units of J_0), $J_A(t)$ is the solid line and $J_B(t)$ is the dashed line. The pulse sequence is applied in the counter-intuitive order. (b) The instantaneous eigenenergy (in units of J) of the lowest four eigenstates of total Hamiltonian (1) through the pulse shown in (a), which were obtained by direct numerical diagonalization of the Hamiltonian. In the weak coupling limit, i.e. $J_0 \ll J$ three lowest states is approximately equivalent to that a triple-quantum-dot system.

and the bus are weak, i.e. $J_0 \ll \Delta$, the Hamiltonian $\hat{\mathcal{H}}_I(t)$ could be treated as perturbation within the time interval $[0, t_{\max}]$. Hence, the effective Hamiltonian can be derived by using perturbation theory at any time during the process, which acts on the subspace $[\mathcal{G}]$ spanned by vectors $|A\rangle$, $|\lambda_0\rangle$, and $|B\rangle$.

In first-order degenerate perturbation theory, the matrix of the effective Hamiltonian with states ordering $\{|A\rangle, |\lambda_0\rangle, |B\rangle\}$ reads

$$\hat{\mathcal{H}}_{\text{eff}} = \begin{bmatrix} -\mu & -\Omega_A(t) & 0 \\ -\Omega_A(t) & -\mu & -\Omega_B(t) \\ 0 & -\Omega_B(t) & -\mu \end{bmatrix} \quad (10)$$

where $\Omega_\alpha(t) = J_\alpha(t) u_0(N_0 - l)$, for $\alpha = A, B$. The eigenstates of the Hamiltonian of the Eq. (10) are

$$|\mathcal{D}_-(t)\rangle = \frac{1}{\sqrt{2}} [\sin \theta(t) |A\rangle - |\lambda_0\rangle + \cos \theta(t) |B\rangle], \quad (11a)$$

$$|\mathcal{D}_0(t)\rangle = \cos \theta(t) |A\rangle - \sin \theta(t) |B\rangle, \quad (11b)$$

$$|\mathcal{D}_+(t)\rangle = \frac{1}{\sqrt{2}} [\sin \theta(t) |A\rangle + |\lambda_0\rangle + \cos \theta(t) |B\rangle], \quad (11c)$$

where we have introduced the mixing angle $\theta(t) = \arctan[J_A(t)/J_B(t)]$, and corresponding energies are $\mathcal{E}_0 = -\mu$, and $\mathcal{E}_\pm = -\mu \mp \sqrt{[\Omega_A(t)]^2 + [\Omega_B(t)]^2}$.

In Fig. 2(b) we plot the four lowest eigenenergies of total Hamiltonian (1) using the pulsing scheme given by Eq. (2) in weak coupling regime. To first order in J_0 , the perturbation Hamiltonian $\hat{\mathcal{H}}_1$ lifts degeneracy of the ground-state manifolds while the excited states $|\lambda_n\rangle$ are unaffected. It is worth mentioning that the energy splitting δ_{eff} of the ground-state subspace is proportional to J_0 . This observation is schematically shown in Fig. 2(b), in which Δ is the typical gap for the unperturbed Hamiltonian \mathcal{H} (i.e., $J_0 = 0$). In fact, the weak coupling limit yields the inequality $\delta_{\text{eff}} \ll \Delta$ which will be equivalent condition for the purposes of perturbation.

One can see that, for weak coupling case, the total system reduces to an effective three-level system that has a non-evolving "dark state", which can serve as the vehicle for population transfer in a STIRAP-like procedure. Note that the angle $\theta(t)$ is totally dependent on the ratio of the two pulse strength and the pulse sequence used here are in the counterintuitive ordering. It is well known that, for the counterintuitive sequence of pulses, in which $J_B(t)$ precedes $J_A(t)$, one has $\theta = 0$ for $t = 0$ and $\theta = \pi/2$ for $t = t_{\text{max}}$. With these results, one can see that the state $|\mathcal{D}_0(t)\rangle$ is $|A\rangle$ initially and goes to $|B\rangle$ finally. The goal here is to study the coherent quantum state transfer from state $|A\rangle$ to state $|B\rangle$ by slowly varying the alternating pulse sequence between QDs A, B and the chain to drive the state transfer. Here we define the transfer distance d to be the number of QDs between the two QDs which the sender A and receiver B are respectively connected with, i.e., $d = 2l + 3$. The transfer fidelity depends on two aspects: (i) the validity of the effective Hamiltonian (10) which is derived from perturbative way and (ii) the dynamics follows the instantaneous eigenstate $|\mathcal{D}_0(t)\rangle$ is whether or not adiabatic. We now investigate these two aspects in the following, and J_0 and μ_0 are scaled by J for simplicity.

Bearing in mind the effective Hamiltonian (10) is the analytic approximation of the total Hamiltonian (1) and this approximation holds when the energy splitting δ_{eff} caused by the $\hat{\mathcal{H}}_{\text{eff}}$ is smaller than the typical gap for the unperturbed Hamiltonian $\hat{\mathcal{H}}$, i.e., $\delta_{\text{eff}} \ll \Delta$. To investigate the range of validity about the above approximation, we compare the instantaneous eigenstate $|\mathcal{D}_0(t)\rangle$ at time $t = t_{\text{max}}/2$ of $\hat{\mathcal{H}}_{\text{eff}}$ with the density matrices reduced from the first excited states of the total system. The density

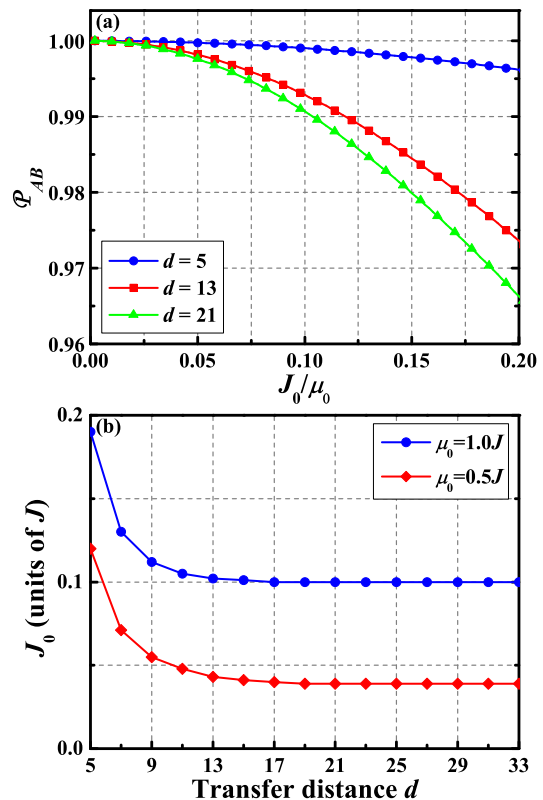


FIG. 3: (Color online) (a) The operator fidelity \mathcal{P}_{AB} as a function of J_0/μ_0 for $d = 5, 13$, and 21 . As the ratio J_0/μ_0 increases the operator fidelity is decreased. (b) The coupling J_0 as a function of d for $\mu_0 = 0.5J$, and $1.0J$ (bottom to top along J_0 axis) under the condition that the operator fidelity greater than 99.5%. The other system parameter is $N = 39$.

matrix corresponding to $|\mathcal{D}_0(t_{\text{max}}/2)\rangle = (|A\rangle - |B\rangle)/\sqrt{2}$ is

$$\begin{aligned} \rho_{AB} &= |\mathcal{D}_0(t_{\text{max}}/2)\rangle \langle \mathcal{D}_0(t_{\text{max}}/2)| \\ &= \frac{1}{2} [|A\rangle \langle A| + |B\rangle \langle B| - |A\rangle \langle B| - |B\rangle \langle A|] \quad (12) \end{aligned}$$

Moreover, we assign the state $|\Psi_1(t_{\text{max}}/2)\rangle$ denotes the instantaneous first-excited state for the total Hamiltonian $\hat{\mathcal{H}}(t = t_{\text{max}}/2)$. Then, the operator fidelity is defined as

$$\mathcal{P}_{AB} = \left(\text{Tr} \sqrt{\rho_{AB}^{1/2} \rho_R \rho_{AB}^{1/2}} \right)^2, \quad (13)$$

where $\rho_R = \text{Tr}_M (|\Psi_1(t_{\text{max}}/2)\rangle \langle \Psi_1(t_{\text{max}}/2)|)$, and Tr_M means the trace over the variables of the tight-binding array. \mathcal{P}_{AB} is sensitive to two parameters, i.e., the ratio of J_0/μ_0 and the transfer distance d . In the following discussions, we will investigate how the above external parameters influence the operator fidelity of the dark state. Fig. 3(a) shows the dependence of \mathcal{P}_{AB} on both J_0/μ_0 and d for the system with $N = 39$. We can see that the

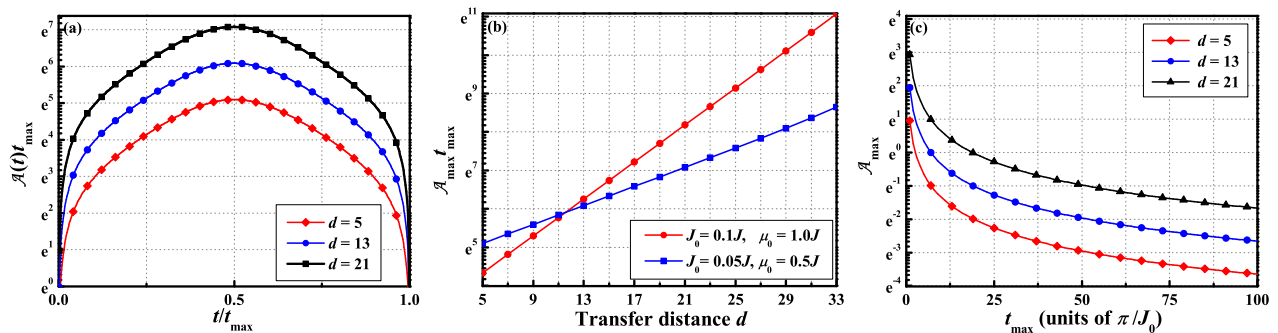


FIG. 4: (Color online) (a) Adiabaticity $\mathcal{A}(t)t_{\max}$ as a function of time in the time interval $t \in [0, t_{\max}]$ corresponding to the pulse shapes as in Eq. (2). The results show that the adiabaticity parameter $\mathcal{A}(t)t_{\max}$ is largest at the crossing point of the two pulses. The parameters we chosen are $N = 39$, $J_0 = 0.05J$, and $\mu_0 = 0.5J$. (b) Maximum adiabaticity $\mathcal{A}_{\max}t_{\max}$ through the protocol as a function of transfer distance d for $N = 39$. The parameters is $J_0 = 0.05J$, $\mu_0 = 0.5J$ (squares) and $J_0 = 0.1J$, $\mu_0 = 1.0J$ (circles). As the transfer distance increases, the adiabaticity parameter increases and the grow of adiabaticity of the large μ_0 is faster than the small one. (c) The maximum adiabaticity parameter \mathcal{A}_{\max} as a function of t_{\max} . As t_{\max} is increased \mathcal{A}_{\max} is decreased, indicating that better fidelity transfer can be achieved for longer total transfer time.

operator fidelity improves by decreasing J_0/μ_0 . Moreover, we note that, increasing the value of d there is a slight shift of \mathcal{P}_{AB} for a given J_0/μ_0 , which means that as the transfer distance increases one need to decrease the ratio J_0/μ_0 if we want high operator fidelity to hold. To obtain high quality of operator fidelity ($\mathcal{P}_{AB} \geq 99.5$), we compute the ratio J_0/μ_0 versus transfer distance d with two different impurity on-site energy μ_0 ; these results are shown in Fig. 3(b). In this figure, one can see that taking $J_0/\mu_0 \leq 0.1$, the effective Hamiltonian agrees very well with the exact solution obtained from numerical calculations. Therefore, we have shown the weak coupling effective Hamiltonian (10) is a very good approximation of the exact model.

B. Adiabatic condition

To realize high-fidelity QST, we require that the system remains in its dark state $|\mathcal{D}_0(t)\rangle$, without loss of population from this state to the neighboring states, i.e., $|\mathcal{D}_{\pm}(t)\rangle$. The adiabaticity parameter defined for this scheme is

$$\begin{aligned} \mathcal{A}(t) &= \frac{|\langle \mathcal{D}_+(t) | \partial_t \hat{\mathcal{H}}_{\text{eff}} | \mathcal{D}_0(t) \rangle|}{|\mathcal{E}_+ - \mathcal{E}_0|^2} \\ &= \frac{|\dot{\Omega}_A(t)\Omega_B(t) - \dot{\Omega}_B(t)\Omega_A(t)|}{\sqrt{2}[\Omega_A^2(t) + \Omega_B^2(t)]^{3/2}}. \end{aligned} \quad (14)$$

The time dependence of the parameter $\mathcal{A}(t)t_{\max}$ is illustrated in Fig. 4(a). Obviously the adiabaticity parameter $\mathcal{A}(t)t_{\max}$ reaches maximum at the crossing point of the two pulses. At this point one has $\Omega_A(t_{\max}/2) = \Omega_B(t_{\max}/2) = J_0 u_0(N_0 - l)/2$ and $\dot{\Omega}_A(t_{\max}/2) = -\dot{\Omega}_B(t_{\max}/2) = \pi J_0 u_0(N_0 - l)/2t_{\max}$. By

using the form of the pulses as given in Eq. (2), the above equation gives rise to the simple form

$$\mathcal{A}_{\max} = \frac{\pi}{J_0 u_0(N_0 - l)t_{\max}}. \quad (15)$$

The analytical expression for maximum adiabaticity is helpful for estimating the quantum state transfer time t_{\max} . For adiabatic evolution of the system we require $\mathcal{A}_{\max} \ll 1$. According to Eq. (15), the total transfer time should satisfy $t_{\max} \gg \pi/[J_0 u_0(N_0 - l)]$. In Fig. 4(b) we present the dependence of the $\mathcal{A}_{\max}t_{\max}$ on the transfer distance d for a system with $N = 39$. Obviously one sees the increase in the adiabaticity parameter with increasing d . Moreover, one can see that the bigger is the μ_0 , the faster is the growth of $\mathcal{A}_{\max}t_{\max}$. The reason is that by increasing μ_0 , the localization effect of Eq. (8) is enhanced. Figure 4(b) also reflects the fact that the optimal transfer time needs to be increased with increasing d . The smaller the μ_0 is, the slower the growth rate will be. Furthermore, the dependence of the adiabaticity parameter on the total protocol time t_{\max} is plotted in Fig. 4(c). With longer t_{\max} , and hence lower \mathcal{A}_{\max} , the transported electron is more likely to remain in the desired $|\mathcal{D}_0(t)\rangle$ state resulting in better fidelity transfer.

C. Coherent state transfer

To simulate the analog of STIRAP protocol we initialize the device so that the particle occupies site $|A\rangle$ at $t = 0$, i.e., the total initial state is $|\Psi(0)\rangle = |A\rangle$, and apply the alternating pulse sequence [see Eq. (2)] in the counterintuitive order. The evolution of the wave function is described by Schrödinger equation

$$i \frac{\partial}{\partial t} |\Psi(t)\rangle = \hat{\mathcal{H}}_{\text{eff}} |\Psi(t)\rangle, \quad (16)$$

which creates a coherent superposition: $|\Psi(t)\rangle = c_A(t)|A\rangle + c_0(t)|\lambda_0\rangle + c_B(t)|B\rangle$. Substituting the super-

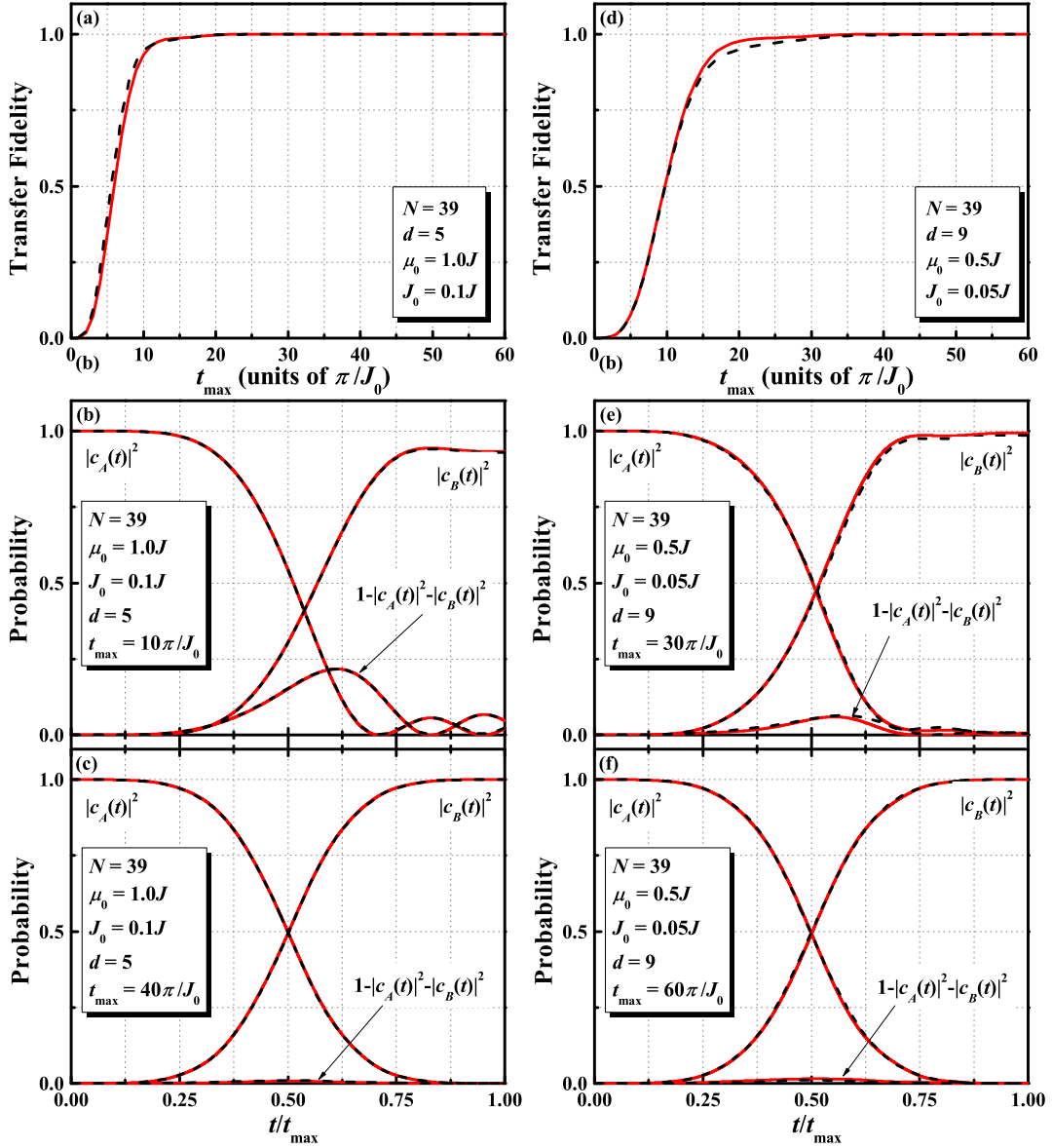


FIG. 5: (Color online) (a) The transfer fidelity F as a function of t_{\max} (in units of π/J_0) for $d = 5$. The parameters we take is $N = 39$, $\mu_0 = 1.0J$, and $J_0 = 0.1J$. The red solid curves correspond to the approximate results via perturbation theory and black dotted curves are the exact numerical results for the complete Hilbert space. (b) The time evolution of the probabilities induced by the pulses in Fig. 2(a) for $d = 5$ and $t_{\max} = 10\pi/J_0$. (c) is the same as (b) but for $t_{\max} = 40\pi/J_0$. (d) The same as in (a), but for $d = 9$, $\mu_0 = 0.5J$, and $J_0 = 0.05J$. (e)-(f) is same as (b)-(c) but for $d = 9$. To get high fidelity transfer, more time is required for longer transfer distance.

position form of $|\Psi(t)\rangle$ into the Schrödinger equation, we get equations of motion for the probability amplitudes

$$\begin{aligned} i\dot{c}_A(t) &= -\Omega_A(t)c_0(t), \\ i\dot{c}_0(t) &= -\Omega_A(t)c_A(t) - \Omega_B(t)c_B(t), \\ i\dot{c}_B(t) &= -\Omega_B(t)c_0(t), \end{aligned} \quad (17)$$

where the dot denotes the time derivative.

A measure of the quality of this protocol after the pulse sequences is given by the transfer fidelity

$$F = |\langle B | \Psi(t_{\max}) \rangle|^2 = |c_B(t_{\max})|^2. \quad (18)$$

To investigate QST between QDs A and B , we numerically solve the time-dependent Schrödinger equation for the multi-dot system with $N = 39$. Here we compare the results obtained from two alternative approaches. In the first case, we numerically integrated Eq. (16) with the initial condition $|\Psi(0)\rangle = |A\rangle$. In the second case, we adopt total Hamiltonian (1) to replace the effective Hamiltonian and we perform a numerical simulation using the total Hamiltonian. In this case the computation takes place in full Hilbert space with basis $\{|A\rangle, |1\rangle, |2\rangle, \dots, |N\rangle, |B\rangle\}$. Fig. 5(a) shows transfer fi-

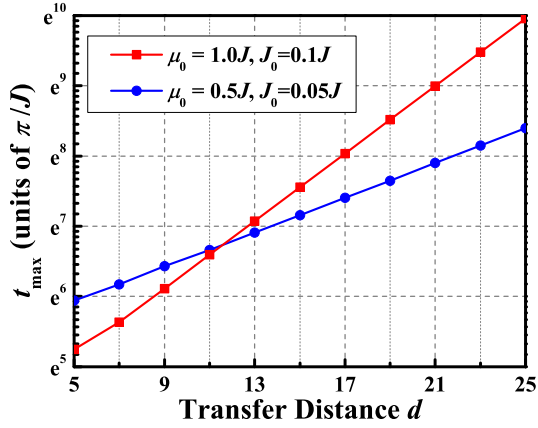


FIG. 6: (Color online) The plot of distance dependence of transfer time t_{\max} for a chosen tolerable transfer error $1 - F = 0.5\%$. The lines are only guides to the eyes. Notice the exponential increase of t_{\max} as a function of the distance. In order to make results comparable, all times are scaled in units of π/J .

delity F as a function of t_{\max} for $d = 5$, $\mu_0 = 1.0J$ and $J_0 = 0.1J$. If we choose $t_{\max} \geq 19\pi/J_0$, the transfer fidelity F will be larger than 99.5%. To illustrate the process of QST, we exhibit in Fig. 5(b) and 5(c) the time evolution of the probabilities. We get perfect state transfer if we choose the transfer time longer enough and the populations on the QD A and QD B are exchanged in the expected adiabatic manner. For the case $d = 9$ with $\mu_0 = 0.5J$ and $J_0 = 0.05J$, it is shown in Fig. 5(d)-(f) that to ensure $F \geq 99.5\%$ the optimal transfer time is about $31\pi/J_0$. For comparison, we also plot in Fig. 5 the result of the exact numerical results (dashed curves) for the full Hilbert space calculation. Obviously, our three-state effective Hamiltonian describes the quantum state evolution very well.

In order to provide the most economical choice of total transfer time t_{\max} for reaching high transfer efficiency, we perform numerical analysis of the relation between t_{\max} and d . For a given tolerable transfer error $1 - F = 0.5$, we plot in Fig. 6 the minimum time varies as a function of transfer distance d . Clearly, the time required for near-perfect transfer depends on d in an exponential fashion. Intuitively, this behavior results from the fact that the ground state of medium Hamiltonian $\hat{\mathcal{H}}_M$ is exponentially localized due to the existence of defect μ_0 , leading to the exponential decrease of the energy splitting δ_{eff} as d increases; and this effect is stronger for larger μ_0 and weaker for smaller μ_0 . In these sense, the negative effects of t_{\max} on the transfer distance can be partially compensated by reducing the defect energy μ_0 . It is conceivable that t_{\max} will scale linearly with d in the limit $\mu_0 \rightarrow 0$.

D. Robustness of state transfer

We have shown that under appropriate system parameters, the total Hamiltonian $\hat{\mathcal{H}}$ can be mapped to a three-level effective Hamiltonian $\hat{\mathcal{H}}_{\text{eff}}$, which establish an effective STIRAP pathway for realizing long-range QST. Not only efficiency but also robustness against technical and fundamental noise is important for a scheme to be applicable in quantum-information processing and quantum computing. There are two central concerns for the QST protocol in experiments, decoherence and imperfect experimental implementations.

In this section, we are going to consider an realistic model which is more close to experimental implementation and analyze the robustness of this scheme to unavoidable imperfections. In particular, we assume that the Hamiltonian has a random but constant offset fluctuation in the couplings, i.e., replacing the couplings in Eq. (1b) with $J \rightarrow J(1 + \delta\epsilon_j)$. The total Hamiltonian is therefore

$$\hat{\mathcal{H}}' = \sum_{j=1}^{N-1} -J(1 + \delta\epsilon_j) |j\rangle \langle j+1| - \frac{\mu_0}{2} |N_0\rangle \langle N_0| - \frac{\mu}{2} (|A\rangle \langle A| + |B\rangle \langle B|) - J_A(t) |A\rangle \langle N_0 - l| - J_B(t) |B\rangle \langle N_0 + l| + \text{h.c.}, \quad (19)$$

where δ is the maximum coupling offset bias relative to J ; ϵ_j is drawn from the standard uniform distribution in the interval $[-1, 1]$ and all ϵ_j are completely uncorrelated with all sites along the medium chain.

Due to the existence of imperfections, the former effective Hamiltonian (10) is no longer hold. We now consider the two effects together with the master equation [18]

$$\dot{\rho}(t) = -i [\hat{\mathcal{H}}'(t), \rho(t)] - \Gamma \{\rho(t) - \text{diag}[\rho(t)]\}, \quad (20)$$

where Γ is the pure dephasing reate. To determine the

robustness of the perturbed situation, we numerically integrate above equation with the electron initialized in QD- A to be transported: $\rho(t=0) = |A\rangle \langle A|$. At the end of the computation ($t = t_{\max}$), we obtain the density matrix $\rho(t_{\max})$. The problem in the following we concern will be to evaluate the transfer fielyty

$$\mathcal{F} = \text{Tr}[\rho(t_{\max}) \rho_B] \quad (21)$$

where $\rho_B = |B\rangle \langle B|$.

Setting $\mu_0 = 1.0J$, $J_0 = 0.1J$, and $d = 5$, figure 7(a)

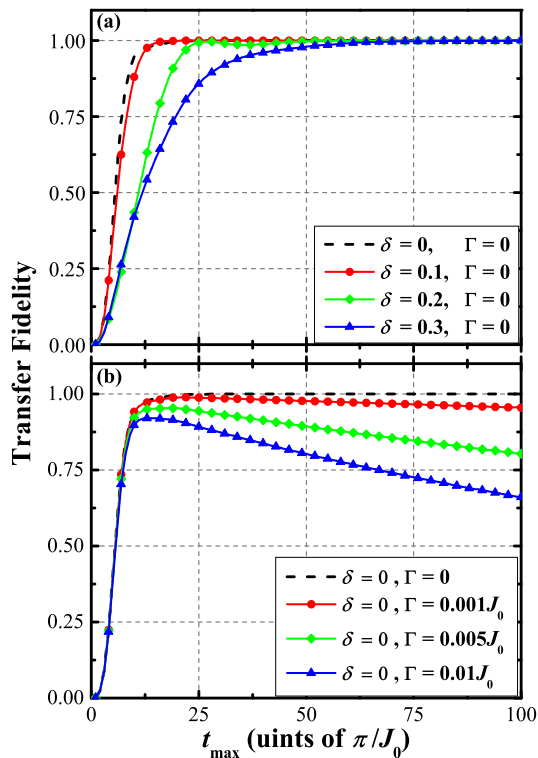


FIG. 7: (Color online) Transfer fidelity \mathcal{F} as a function of total transfer time t_{\max} for (a) $\Gamma = 0$ and different values of δ ; (b) $\delta = 0$ and different values of Γ . The parameter values we take is $N = 39$, $\mu_0 = 1.0J$, $J_0 = 0.1J$, and $d = 5$.

shows the solutions of the master equation (20) for $\Gamma = 0$ and for different values of maximum coupling offset δ , in which we have chosen to report the transfer fidelity \mathcal{F} as a function of the total duration time t_{\max} of QST. Bearing in mind that a total duration time t_{\max} greater than $19\pi/J_0$ can guarantee the perfect state transfer for ideal case (i.e., $\Gamma = 0$ and $\delta = 0$). As expect, this approach is robustly insensitive to weak fluctuations ($\delta \leq 0.1$) of the couplings. By increasing δ , the negative effects on transfer fidelity become more and more pronounced, and this negative influence can be compensated when the duration of the process is chosen to be long enough. This means that the scheme allows one to increase the transfer fidelity arbitrarily close to unity, without the need for a precise control of the couplings. In Fig. 7(b), we show the effects of dephasing on transfer fidelity. When dephasing is considered, perfect QST cannot be achieved. For optimum value of t_{\max} , transfer fidelity has a maximum value \mathcal{F}_{\max} which decreases when Γ is increased. For $\Gamma = 0.001J_0$, the optimum value for t_{\max} is $t_{\max} = 21\pi/J_0$ with $\mathcal{F}_{\max} = 0.99$. When $\Gamma = 0.005J_0$, \mathcal{F}_{\max} reaches 0.95 at $t_{\max} = 18\pi/J_0$. The optimum value of t_{\max} is slightly shorter than ideal case because dephasing will have more time to destroy the coherent transfer

as t_{\max} increases.

IV. SUMMARY

The central idea of this work is to model a solid-state adiabatic quantum communication protocol suitable for high fidelity robust multiple-range QST and quantum information swapping. It has been shown that high fidelity two-way QST can be realized at various different distances by introducing an N -site tight-binding QD array as quantum data bus. We first demonstrate that the tight-binding chain with a diagonal defect has a non-vanishing energy gap above the ground state in the single-particle subspace; and this defect produces an eigenstate exponentially localized at the defect. Our approach to realize high-fidelity QST is based on the fact that the two information exchange QDs are resonantly coupled to the zeroth eigen-mode of the quantum data bus. By treating the weak coupling as perturbation, the system can be reduced to a three-level system by the first-order terms in the perturbative expansion, which enables us to perform an effective three-level STIRAP. Then we present that it is possible to transfer an arbitrary quantum state driven by adiabatically modulating two side couplings. For proper choices of the system parameters, perfect adiabatic QST can be obtained, which has been confirmed by exact numerical simulations. Moreover, for an increasing transfer distance, we find that the evolution time displays an exponential dependence on the transfer distance. However, this negative effect can be suppressed by reducing the defect energy μ_0 . Finally, the robustness of the scheme to fabrication disorder and dephasing is numerically demonstrated.

Comparing to the existing long-rang QST schemes, our proposal has the following advantages: i) the requirement of tunnelling control are minimized. This means that our scheme provides an efficient alternative long-range QST scheme without performing many tunnelling operations. ii) different transfer distance can be achieved by changing the connecting site of two side QDs, and no additional QDs are needed. Our proposal provides a novel scheme to implement ordinary STIRAP protocols in many-body solid-state systems in the realization of high-fidelity multiple-range QST.

Acknowledgements

This work is supported by the National Natural Science Foundation of China (Grant Nos. 11105086, 11204162), and the SDUST Research Funds (2012KYTD103 and 2014JQJH104), as well as the National Science Foundation through awards PHY-1505189 and INSPIRE PHY-1539859.

-
- [1] M. A. Nielsen and I. L. Chuang, *Quantum Computation and Quantum Information* (Cambridge Univ. Press, 2000); and J. Preskill, *Quantum Information and Computation*, Caltech Lecture Notes for Ph219/CS219.
- [2] S. Bose, *Contemporary Physics*, **48**, 13 (2007).
- [3] S. Bose, *Phys. Rev. Lett.* **91**, 207901 (2003).
- [4] M. Christandl, N. Datta, A. Ekert and A. J. Landahl, *Phys. Rev. Lett.* **92**, 187902 (2004).
- [5] V. Subrahmanyam, *Phys. Rev. A* **69**, 034304 (2004).
- [6] D. Burgarth and S. Bose, *Phys. Rev. A* **71**, 052315 (2005).
- [7] Ying Li, Tao Shi, Bing Chen, Zhi Song, and Chang-Pu Sun, *Phys. Rev. A* **71**, 022301 (2005).
- [8] Tao Shi, Ying Li, Zhi Song, and Chang-Pu Sun, *Phys. Rev. A* **71**, 032309 (2005).
- [9] M. Paternostro, G. M. Palma, M. S. Kim, and G. Falci, *Phys. Rev. A* **71**, 042311 (2005).
- [10] Xiao-Feng Qian, Ying Li, Yong Li, Z. Song, and C. P. Sun, *Phys. Rev. A* **72**, 062329 (2005).
- [11] Alastair Kay, *Phys. Rev. Lett.* **98**, 010501 (2007).
- [12] C. Di Franco, M. Paternostro, and M. S. Kim, *Phys. Rev. Lett.* **101**, 230502 (2008).
- [13] Giulia Gualdi, Vojtech Kostak, Irene Marzoli, and Paolo Tombesi, *Phys. Rev. A* **78**, 022325 (2008).
- [14] Bing Chen, Yong Li, Z. Song, C. P. Sun, *Annals of Physics* **348**, 278 (2014).
- [15] S. Lorenzo, T. J. G. Apollaro, S. Paganelli, G. M. Palma, and F. Plastina *Phys. Rev. A* **91**, 042321 (2015).
- [16] Chiranjib Mitra, *Nature Physics* **11**, 212-213 (2015).
- [17] K. Bergmann, H. Theuer, and B. W. Shore, *Rev. Mod. Phys.* **70**, 1003 (1998).
- [18] A. D. Greentree, J. H. Cole, A. R. Hamilton, and L. C. L. Hollenberg, *Phys. Rev. B* **70**, 235317 (2004).
- [19] K. Eckert, M. Lewenstein, R. Corbalán, G. Birkel, W. Ertmer, and J. Mompart, *Phys. Rev. A* **70**, 023606 (2004).
- [20] N. V. Vitanov, and B. W. Shore, *Phys. Rev. A* **73**, 053402 (2006).
- [21] S. McEndoo, S. Croke, J. Brophy, and Th. Busch, *Phys. Rev. A* **81**, 043640 (2010).
- [22] W. Merkel, H. Mack, M. Freyberger, V. V. Kozlov, W. P. Schleich, and B. W. Shore, *Phys. Rev. A* **75**, 033420 (2007).
- [23] S. Longhi, *J. Phys. B: At. Mol. Opt. Phys.* **40**, F189 (2007).
- [24] S. Longhi, G. Della Valle, M. Ornigotti, and P. Laporta, *Phys. Rev. B* **76**, 201101(R) (2007).
- [25] G. Della Valle, M. Ornigotti, T. T. Fernandez, P. Laporta, S. Longhi, A. Coppa, and V. Foglietti, *Appl. Phys. Lett.* **92**, 011106 (2008).
- [26] K. Eckert, J. Mompart, R. Corbalán, M. Lewenstein, and G. Birkel, *Opt. Commun.* **264**, 264 (2006).
- [27] T. Opatrny, and K. K. Das, *Phys. Rev. A* **79**, 012113 (2009).
- [28] T. Morgan, B. O'Sullivan, and Th. Busch, *Phys. Rev. A* **83**, 053620 (2011).
- [29] T. Ohshima, A. Ekert, D. K. L. Oi, D. Kaslizowski, L. C. Kwek, e-print arXiv:quant-ph/0702019.
- [30] A. D. Greentree and Belita Koiller, *Phys. Rev. A* **90**, 012319 (2014).
- [31] J. Fabian and U. Hohenester, *Phys. Rev. B* **72**, 201304(R) (2005).
- [32] C. J. Bradly, M. Rab, A. D. Greentree, and A. M. Martin, *Phys. Rev. A* **85**, 053609 (2012).
- [33] E. M. Graefe, H. J. Korsch, and D. Witthaut, *Phys. Rev. A* **73**, 013617 (2006).
- [34] M. Rab, J. H. Cole, N. G. Parker, A. D. Greentree, L. C. L. Hollenberg, and A. M. Martin, *Phys. Rev. A* **77**, 061602(R) (2008).
- [35] V. O. Nesterenko, A. N. Nikonov, F. F. de Souza Cruz, and E. L. Lapolli, *Laser Phys.* **19**, 616 (2009).
- [36] J. A. Vaitkus and A. D. Greentree, *Phys. Rev. A* **87**, 063820 (2013).
- [37] A. D. Greentree, S. J. Devitt, and L. C. L. Hollenberg, *Phys. Rev. A* **73**, 032319 (2006).
- [38] L. M. Jong, A. D. Greentree, V. I. Conrad, L. C. L. Hollenberg, and D. N. Jamieson, *Nanotechnology* **20**, 405402 (2009).
- [39] L. C. L. Hollenberg, A. D. Greentree, A. G. Fowler, and C. J. Wellard, *Phys. Rev. B* **74**, 045311 (2006).
- [40] S. Longhi, *Annals of Physics* **348**, 161 (2014).
- [41] L. M. Jong, and A. D. Greentree, *Phys. Rev. B* **81**, 035311 (2010).
- [42] R. Menchon-Enrich, S. McEndoo, Th. Busch, V. Ahufinger, and J. Mompart, *Phys. Rev. A* **89**, 053611 (2014).
- [43] David Petrosyan, Georgios M. Nikolopoulos, and P. Lambropoulos, *Phys. Rev. A* **81**, 042307 (2010).
- [44] Umer Farooq, Abolfazl Bayat, Stefano Mancini, and Sougato Bose, *Phys. Rev. B* **91**, 134303 (2015).
- [45] E. Ferraro, M. De Michielis, M. Fanciulli, and E. Prati, *Phys. Rev. B* **91**, 075435 (2015).